HHS Public Access

Author manuscript

ACS Nano. Author manuscript; available in PMC 2015 June 15.

Published in final edited form as:

ACS Nano. 2014 June 24; 8(6): 6047–6055. doi:10.1021/nn501312q.

Digital Sensing and Sizing of Vesicular Stomatitis Virus Pseudotypes in Complex Media; A Model for Ebola and Marburg Detection

George G. Daaboul[#1], **Carlos A. Lopez**[#1], **Jyothsna Chinnala**[1], **Bennett B. Goldberg**[1,2,3], **John H. Connor**[4,5], and **M. Selim Ünlü**[1,2,3,*]

[1]Electrical & Computer Engineering Dept., Boston University, Boston, MA 02215

[2]Biomedical Engineering Dept., Boston University, Boston, MA 02215

[3]Physics Department, Boston University, Boston, MA 02215

[4]Department of Microbiology and National Emerging and Infectious Diseases Laboratories, Boston University School of Medicine, Boston, MA 02118

[5]Boston University Photonics Center, Boston University, Boston, MA 02215

[#] These authors contributed equally to this work.

Abstract

Rapid, sensitive, and direct label-free capture and characterization of nanoparticles from complex media such as blood or serum will broadly impact medicine and the life sciences. We demonstrate identification of virus particles in complex samples for replication-competent wild-type vesicular stomatitis virus (VSV), defective VSV, and Ebola- and Marburg-pseudotyped VSV with high sensitivity and specificity. Size discrimination of the imaged nanoparticles (virions) allows differentiation between modified viruses having different genome lengths and facilitates a reduction in the counting of non-specifically bound particles to achieve a limit-of-detection (LOD) of 5×10^3 pfu/mL for the Ebola and Marburg VSV pseudotypes. We demonstrate the simultaneous detection of multiple viruses in a single sample (composed of serum or whole blood) for screening applications and uncompromised detection capabilities in samples contaminated with high levels of bacteria. By employing affinity-based capture, size discrimination, and a “digital” detection scheme to count single virus particles, we show that a robust and sensitive virus/nanoparticle sensing assay can been established for targets in complex samples. The nanoparticle microscopy system is termed the Single Particle Interferometric Reflectance Imaging Sensor (SP-IRIS) and is capable of high-throughput and rapid sizing of large numbers of biological nanoparticles on an antibody microarray for research and diagnostic applications.

[*]**Corresponding Author**: selim@bu.edu.

Supporting Information. Figure S1-S2. This material is available free of charge *via* the Internet at http://pubs.acs.org.

Author Contributions

The manuscript was written through contributions of all authors. All authors have given approval to the final version of the manuscript.

Keywords

Single Virus; Viral Hemorrhagic Fevers; Label Free; Biosensor

Within the last decade, events involving influenza pandemics, development and intentional dissemination of highly virulent biowarfare agents, and deadly global outbreaks of viral hemorrhagic fevers (VHFs) contributed to concerns of potential bioterrorism and outbreak episodes and have driven the demand for rapid and simple virus sensing technologies as a way to provide effective diagnosis of infection.[1-45, 6] To successfully detect and contain the spread of a pathogen at the point-of-need, such technologies must be fast, sensitive, and field deployable. Polymerase chain reaction (PCR) is the current gold standard technique for the sensitive identification of many pathogens, however significant sample preparation is required before a nucleic acid target can be amplified, and detection involves the use of fluorescent reporters. Both of these steps pose a barrier to field utility. Often, initial diagnosis of infection with Ebola and Marburg done not at the point of care, but outside of the country.[7, 8] The sensing of single virus particles from whole blood and serum, without the need for sample preparation, would provide a simpler and more direct approach to virus detection and could allow earlier on-site detection of these viruses.

The rapid detection of natural biological nanoparticles like single virions has applications beyond point-of-need diagnostics. The sensing and characterization of specific, low abundance virus populations in complex mixtures can be applied to nanomedicine, virology, and vaccine development. For example, many different types of viruses are now being investigated as vehicles for targeted cancer therapies.[9-13] In the fields of virology and vaccine development, genetically modified viruses are being studied to understand pathogenesis and to create vaccines and treatments for diseases with high mortality and morbidity rates, but no available prophylactic measures.[14-17] Synthetic nanoparticles are also playing an increasingly important role in medicine and the life sciences; many types of synthetic particles are being developed to improve both drug delivery and medical imaging for cancer treatment and diagnostics.[18, 19] The characterization of individual nanoparticles based on their size and surface properties would help to elucidate the efficacy of their intended function in many of these applications.

Technologies that interrogate nanoparticles based on morphological and functional characteristics generally utilize optical, electrical, or mechanical transduction methods.[20] Optical or mechanical techniques that rely on resonant structures have limited throughput and cannot quantify large populations of heterogeneous mixtures.[2122, 23] Electrical impedance measurements across a porous membrane can characterize a large population of nanoparticles but do not allow users to probe the expression or function of membrane-bound proteins on the particle.[24] Wide-field on-chip microscopy of single nanoparticle is an emerging approach that allows detection of nanoparticles over a large field-of-view.[25, 26] However, these new technologies have not yet shown specific capture of viral pathogens. A technique combining affinity-based particle capture with high-throughput measurements could effectively evaluate population homo- and heterogeneity and the presence of functional surface ligands.

To address the need for a simple method of capturing and analyzing single nanoparticles from complex solutions, we have developed an interferometric measurement technique that utilizes antibody microarrays for high affinity target capture, isolation, and screening. In recent publications we have shown that SP-IRIS can individually count and size virus particles captured specifically on the surface from serum.[27] In this article we extend the study to demonstrate direct detection from whole blood with contaminants like bacterial agents for three virus types with high sensitivity and specificity. Additionally, we show that SP-IRIS can not only discriminate between virions and non-specific or background nanoparticles, but also discrimination between similar viruses that differ by as little as 20 nm in size.

Results

Sensing platform for the capture, sizing, and identification of intact virions from complex media

The Single Particle Interferometric Reflectance Imaging Sensor (SP-IRIS) is a wide-field imaging technique that allows detection of individual nanoparticles bound to the Si/SiO_2 sensor surface. The imaging system consist of a simple, low-cost custom microscope which utilizes LEDs for illumination, 50× 0.8 NA objective, and a CCD camera shown in supporting information FigS1. For digital virus detection the microarray architecture shown in Figure 1a was designed to capture whole virus particles on the sensor surface from solution by utilizing monoclonal antibodies tethered to a non-fouling copolymer coated onto the oxide surface of a SiO_2/Si substrate. The sensor substrate is optimized for interferometric reflectance imaging of viruses and nanoparticles in the range of 60-200nm.[28,29] Antibodies, which specifically recognize the VSV glycoprotein, were deposited on the layered substrate as approximately 150 μm diameter spots. Additional antibodies recognizing either Ebola (EBOV) or Marburg virus (MARV) glycoproteins were also arrayed onto the surface to control for any non-specific binding. Figure 1b shows color-coded pre-incubation spot images for each type of antibody.

Following sample incubation, individual particles bound to the sensor surface were identified and subsequently characterized through a sizing model relating measured signal intensity to nanoparticle size. Earlier work on this microscopy system has confirmed the relationship between optical signal and low-index nanoparticle size.[20, 28] To identify viruses bound to the microarray, we compare images of the anti-VSV spots before and after exposure to VSV, as displayed in the representative images in Figure 1b for before (left) and after (right) incubation with the virus sample. After incubation with 10^5 pfu/mL VSV in 100% fetal bovine serum (FBS), the captured viruses on the sensor surface appear as discrete, dot-like objects. Each dot-like object in the image (for each type of antibody) is analyzed for contrast and width and compared to the sizing curve calculated from a forward model (Figure 1c, left). The resulting histograms (Figure 1c, right) for pre- and post exposure conditions are subtracted to yield the number of virus particles bound following incubation with the sample of interest. Based on the known average size of vesicular stomatitis virions as measured by electron microscopy (an ellipsoid of approximately 70 nm by 180 nm)[30], we estimate the response to be similar to a spherical nanoparticle with a

diameter of approximately 110 nm. As can be seen in the right panel of Figure 1c, the observed peak of the histogram of captured VSV is close to 110 nm. Background reduction is possible, through elimination of non-specifically bound particles of a different size than the target virus. The filter window is established by running an experiment with a relatively high concentration of the target virus to establish the expected size distribution histogram. The dashed green rectangle in figure 1c shows the filter window for VSV, the width of the window is selected to encompass the VSV distribution. Particles that are outside the filter window are eliminated to reduce assay noise. In this way, we can improve sensitivity and specificity of affinity-based capture through particle size discrimination.

Virus population characterization through SP-IRIS capture and sizing capabilities

The ability to capture nanoparticles using affinity-based methods combined with size determination provides a unique method to characterize particle size distributions in a virus population. Previously, the ability to determine virus particle size was largely restricted to electron microscopy that required significant purification and technique expertise. Here we tested the efficacy and ability of our platform to both capture and size select targets using a set of virions of varying sizes and glycoprotein expression profiles.

We investigated whether the SP-IRIS platform was sensitive enough to identify viruses that contain additional genetic material. Recombinant viruses that contained genetic material from viral hemorrhagic fever viruses (Ebola or Marburg virus glycoproteins) were inserted with genes for glycoproteins that extended the length of the VSV genome by about 500 bp. Cryo-EM study of VSV structure shows that the viral RNA forms the backbone for the ribbon like structure of the nucleoprotein which wraps in a helical structure to form the bullet shaped nucleocapsid. [31, 32] Therefore, as genetic material is removed or added to the VSV genome the length of the virus is predicted to scale linearly. Figure 2a is a plot of the calculated SP-IRIS response for cylindrical particles with a fixed diameter of 75nm and varying length. The SP-IRIS response for cylindrical particles was generated using the same model used for spherical particles by changing the expression defining the polarizability of the particle to an ellipsoid as explained by Daaboul et al.[28] Genetically modified VSV of varying genome length were captured on the SP-IRIS sensor using antibodies directed against glycoproteins expressed on the virus surface. Figure 2b shows the measured median length of defective interfering particles of VSV (DIP), VSV, Marburg pseudotyped VSV (MARV), Ebola Zaire pseudotyped VSV (EBOV), and Ebola Zaire/Sudan pseudotyped VSV (EBOV-ZS). The results from SP-IRIS measurements for the different VSV-based virions, confirms the predicted linear length dependence on genome size. These results show the capability to classify virus size without prior purification. This ability can enable the study of particle size variation in both lab-adapted and clinical virus samples.

Figure 3 demonstrates our ability to discriminate between wild type VSV and defective interfering particles of VSV in a mixture. Defective interfering particles (DIPs) are a truncated, non-infectious particle known to have a significantly reduced genome size that is naturally produced by many negative strand RNA viruses, and their presence has been implicated in reducing the pathogenicity of many viruses.[33-35] We compared a VSV DIP particle of approximately 6 kb to wild type VSV of 11 kb. Figure 3a-b shows the measured

average diameter of VSV and DIP using SP-IRIS to be 105 nm and 80 nm, respectively. To determine if VSV and DIP can be differentiated using SP-IRIS a mixture of 80% DIP and 20% VSV was incubated on an SP-IRIS sensor. Figure 3c shows the histogram of the detected and sized nanoparticles on the anti-VSV spots following incubation with the virus mixture. The data are best fit by two distributions with peak diameters of 110nm and 82nm, demonstrating distinguishability of the two different virus particle sizes. In addition, the smaller DIP with the greater concentration also yielded the larger number of particles. In principle, we can distinguish among several distinct distributions when the width of each distribution is narrower than the peak size separation.

High-throughput size determination of affinity-captured targets can simultaneously provide valuable information not only on particle morphology, but also on ligand binding characteristics. Pseudotyped VSV variants with different surface glycoproteins are being developed as vaccines to protect against VHFs like the Ebola and Marburg viruses.[14, 16, 36-42] Knowledge of the functionality and expression levels of the different glycoproteins on each of the genetically engineered viruses can help in characterizing their vaccine potential and efficacy.

Virus detection assay sensitivity, specificity, and repeatability for wild type and pseudotyped VSV

To assess the specificity and performance of SP-IRIS for rapid virus diagnostics we determined the assay limit-of-detection (LOD) for VSV spiked in FBS, human whole blood, and serum containing E.coli K12. Individual spotted chips (using the microarray architecture in Figure 1a) were incubated with decreasing concentrations of virus diluted in FBS. Figure 4a shows the results for detection in serum samples containing the wild-type virus with concentrations from 10^7 down to zero pfu/mL. The inset of Figure 4a shows the linear detection range for SP-IRIS for the concentration range of 10^4 to 10^7 pfu/mL. The threshold count of ~30 particles per spot for detection of VSV (represented by the horizontal dashed line in the inset) was determined from the mean plus three standard deviations of particle counts across all anti-VSV spots for the blank sample (serum without virus). The limit-of-detection established for virus counts at this threshold was determined to be 8×10^4 pfu/mL, a sensitivity similar to or better than what has been reported for other antibody-based diagnostic approaches.[43, 44]

To test the specificity of virus detection in a contaminated sample, we repeated the experiment with high levels of bacteria present. A second set of virus dilutions were prepared identically to the one shown in Figure 4a, however, 10^6 colony-forming units/mL (cfu/mL) of E. coli K12 was present in each of the dilutions. The results shown in Figure 4b present the responses for anti-VSV spots in serum *versus* in serum with bacteria as the detection media at each virus concentration. A nearly identical correlation was observed between the two samples (a linear fit to the data produced a line with a slope of 1.05) indicating that at each virus concentration, similar counts were observed between normal serum and serum with bacteria. The particle counts determined on control spots were also observed to be the same between normal FBS and serum with bacteria samples indicating

that an increase in background noise is not observed when high levels of bacteria are present in the sample.

We extended the potential interference with contaminated samples by exploring the efficacy of the SP-IRIS assay to detect virions present in human whole blood. The use of blood can pose problems for molecular assays because the presence of a large and diverse set of macromolecules and biological nanoparticles can contribute significantly to assay noise.[45-47] Figure 4c shows the results for VSV detection in whole blood samples. For incubation in blood, a concentration-dependent response for the anti-VSV spots was observed as seen in samples incubated with serum. Additionally, the number of detected virus particles at each concentration was similar to those obtained for serum dilutions. The LOD determined from the mean plus three standard deviations of the control (blank) sample was found to be identical to serum samples (8×10^4 pfu/mL) indicating that the current assay can maintain equal detection sensitivity between serum and whole blood.

Duplexed screening of model viral hemorrhagic fever viruses

Detection platforms that leverage multiplexed assays are valuable in screening applications. To investigate the multiplexing capacity of SP-IRIS we tested the simultaneous detection of multiple model hemorrhagic fever viruses in a mixed sample. The responses for samples containing a single form of pseudotyped virus (EBOV or MARV) were compared with samples that contained a mixture of both EBOV and MARV. To further increase the complexity of the samples, single and dual virus solutions were prepared in serum containing 10^6 cfu/mL of E. coli K12 as before. Figure 5a shows the results for the simultaneous detection of EBOV and MARV. The concentration of MARV was kept constant at 10^5 pfu/mL while the EBOV pseudotype was serially diluted. In the case of samples that contained only EBOV, minimal counts were observed for the Marburg-specific antibody spots indicating negligible cross-reactivity. For the mixed virus samples, as expected, antibody spots that were specific for MARV produced nearly constant virus counts across all samples while the Ebola-specific antibodies showed a dilution dependent response. Supplemental figure S2 shows the results from an analogous experiment where the concentration of the Ebola pseudotype was kept constant, but the concentration of the Marburg pseudotype was changed from zero to 10^6 pfu/mL.

The limit-of-detection for EBOV and MARV in either mixed or single virus samples was 5×10^3 pfu/ml. Figure 5b compares the responses between the anti-EBOV spots for the single and dual virus samples. Again, similar responses are observed for each type of solution across all concentrations tested. We have achieved a high level of sensitivity while maintaining specific detection in complex samples over 4 orders of magnitude in virus concentration. As with single virus wild type VSV samples (Figure 4b), Figure 5c shows the correlation in virus particles detected for the anti-EBOV spots between dual and single virus samples. A strong linear correlation with a slope 0.87 was observed for both types of samples indicating a negligible effect on specific (Ebola pseudotype) detection when Marburg-pseudotyped VSV was present at 10^5 pfu/mL.

Discussion

Here we demonstrate the effective application of a simple approach to imaging nanoparticles that are below the resolution limits for visible light. The ability to detect particles that are below the diffraction limit provides SP-IRIS with single particle sensitivity and the ability to monitor distinct binding events. In some cases, a sensing technique is not limited by the number of molecular targets in a sample, but rather by signal transduction, or the ability to convert an ensemble of individual binding events into a measureable quantity. The detection and counting of individual virus particles provides a way to surpass sensitivity barriers for some ensemble measurements that are limited by the amount of target material present in a sample.

Numerous methods are available to detect viruses. These methods include molecular tests, such as PCR and immunoassays, to culture-based techniques like the plaque assay and generally require significant time, sample preparation, and laboratory resources to achieve high sensitivity and specificity. By combining affinity-based recognition and capture of targets and “digital” sensing (single particle counting and sizing) without the need for sample preparation, we have achieved high sensitivity virus detection in a simple and rapid technique. The SP-IRIS sensor platform can be applied generally to the characterization of biological nanoparticles using an interferometric substrate that can be arrayed with many capture probes for high-throughput analysis. SP-IRIS is the first system to combine direct label-free detection with sizing of individual biological nanoparticles (such as virions) in a microarray technology. The combination of multiplexed affinity capture with single particle counting and sizing offers a unique method for the characterization of functionalized synthetic or biological nanoparticles. An assay based on this technique is not affected by complex biological solutions allowing direct detection of nanoparticles of interest from native media. The simplicity of the detection scheme and ability to directly identify particles makes this a versatile tool that can be used in both the research and clinical diagnostics fields.

The sizing capabilities of SP-IRIS allowed different types of virions to be distinguished based on their genome lengths in a high-throughput manner. Electron microscopy (EM) is often used to image virus particles and determine the size distribution of a virus/nanoparticle population. Though EM has nanometer resolution it is laborious and low-throughput making it difficult to count and size individual virions to yield accurate statistics on populations. SP-IRIS can rapidly characterize thousands of ligand-expressing nanoparticles directly from unprocessed media. Our results on the detection of model virions expressing hemorrhagic fever virus glycoproteins indicate that SP-IRIS can be effective as a point-of-need device for the rapid detection of viral infections under conditions where access to PCR or fluorescent imaging equipment may be limiting. We have demonstrated the detection of surrogate viruses expressing native Ebola and Marburg glycoproteins at high sensitivity (5×10^3 pfu/mL) directly from serum and blood in ~2 hours in the presence of high levels of a bacterial contaminant. The ability to overcome microbial interference offers practical advantages for laboratory-based measurements, particularly in the case of live culture assays where sample contamination can preclude accurate determination of virus type.

Nanoparticle-based imaging reagents and therapeutics will also benefit from high-throughput ligand-expression and sizing characterization. A major challenge in the development of targeted therapeutic nanoparticles is understanding the relationship between efficacy and ligand-expression.[48, 49] The attachment of surface moieties to target different cell types or tissues does not necessarily confer selective binding; often times, conformational disruption or interaction with host proteins can affect the intended function and therefore novel functionalized particles must be characterized for their binding and recognition properties. The results presented here can be extended to other viral or synthetic nanoparticle targets with diameters greater than 60 nm because the SP-IRIS platform utilizes a highly customizable microarray format. Assay versatility can be important when high-throughput characterization of numerous particles types is desired. Endpoint measurements of particle interactions provide valuable information on ligand presence and functionality, however dynamic analysis of association and dissociation rates can provide a more detailed picture of particle binding mechanisms. Currently, we are investigating the real-time monitoring of nanoparticle binding to the sensor surface to better understand interactions with surface receptors at the level of single binding events.

Methods

SP-IRIS instrumentation

SP-IRIS imaging effectively measures the intensity signal for particles relative to the surrounding background. The background normalized intensity values for each particle are referenced to a sizing curve, which is calculated using a theoretical forward model. SP-IRIS utilizes custom software to identify particle-associated intensity peaks in the image (above the noise) and applies a Gaussian filter to remove non-diffraction limited objects in the image.[50]

Microarray sensor preparation

The SP-IRIS sensor substrates were purchased from Silicon Valley Microelectronics. They consist of a silicon substrate with 100 nm of a thermally grown silicon dioxide layer. The SP-IRIS sensors are functionalized with a copolymer with reactive NHS groups to bind antibody probes[29]. Antibody probes were arrayed on the sensor using a Scienion S3 SciFlexArrayer. Arrayed sensors were left overnight for probe (antibody) immobilization then excess, unbound antibody was washed away with 1× PBST (0.1% Tween-20), rinsed with Nanopure filtered water and dried under nitrogen. Arrays were stored at 4° C and used within 1 week. Mouse monoclonal antibody against VSV glycoprotein was produced from hybridoma cells. Mouse monoclonal against Marburg virus glycoprotein was provided to us from Dr. Takada at Hokkaido University. Mouse monoclonal against Ebola-Zaire was provided to us from the United States Army Medical Research Institute of Infectious Diseases.

Virus incubation in serum and whole blood

Virus was serially diluted from stock solutions in cell media for limit-of-detection experiments. For serum experiments, virus titers were confirmed for all dilutions using plaque assays. Fetal bovine serum was purchased from ATCC (#30-2020). Human whole

blood was purchased from Innovative Research, Inc. Blood was collected using 10 mL K_3 EDTA glass vacutainers and was used within 1 week of draw. For whole blood testing, virus was directly spiked into blood samples without any processing. Virus capture experiments were performed in 24 well cell culture plates. The SP-IRIS sensor was placed directly in a well with 1mL of virus solution. The virus solution was incubated with the SP-IRIS sensor for 2 hours on an orbital shaker. After incubation, each sensor substrate was washed 3 times in 1× PBS for 3 minutes, 1 time in 0.1× PBS for 1 minute then rinsed in Nanopure water and dried under nitrogen. Following the wash step, each substrate was imaged on SP-IRIS. We have read sensors up to 1 year after experiment without deterioration in the signal.

Virus creation, preparation, and use

VSV-based viruses expressing Ebola or Marburg glycoproteins were created by inserting the relevant glycoprotein cDNA into an independent transcription start/stop sequence placed in between the M and L genes in a VSV genome where the VSV glycoprotein sequence had been removed. A detailed description of this construction will be provided elsewhere (C. Mire, J. Connor, and T. Geisbert, manuscript in preparation). Briefly, for dual-glycoprotein expressing viruses, each glycoprotein was inserted into a separate viral transcription start/stop sequence in the pAK VSV vector, a kind gift of Andrea Marzi at Rocky Mountain National Labs. The pAK vector contains two open reading frames between the M and L genes of a VSV-based vector.[40] For three glycoprotein-expressing vectors, the pAK vector was modified to contain an additional transcription start/stop site between the N and P proteins. One glycoprotein was inserted into each transcription start/stop site.

Monovalent, divalent, and trivalent viruses were recovered using standard virus recovery procedures[51]. Recovered viruses were plaque purified and the expression of Ebola and Marburg virus glycoprotein was confirmed by western blotting using glycoprotein-specific proteins. Virus stocks were prepared using Vero cells cultured in DMEM supplemented with 10% FBS, as described previously.[52] Virus titers were determined by standard plaque assay methods.

Supplementary Material

Refer to Web version on PubMed Central for supplementary material.

ACKNOWLEDGMENT

We gratefully acknowledge the Hensley and Olinger laboratories at USAMRIID for their kind sharing of antibodies against Marburg and Ebola, and the Takada laboratory (Hokkaido University) for sharing antibodies against Marburg, as well as the Yin laboratory for sharing the DIP VSV (University of Wisconsin). We also thank Natalia Mamaeva and Maohua Lei for their technical expertise in preparing various virus stocks. GGD gratefully acknowledges financial support from the Center for Integration of Medicine and Innovative Technology (CIMIT). This work was supported by R01AI1096159 to JHC and MSU.

REFERENCES

1. MacNeil A, Farnon EC, Morgan OW, Gould P, Boehmer TK, Blaney DD, Wiersma P, Tappero JW, Nichol ST, Ksiazek TG, et al. Filovirus Outbreak Detection and Surveillance: Lessons from Bundibugyo. J Infect Dis. 2011; 204(Suppl 3):S761–7. [PubMed: 21987748]

2. Blendon RJ, Benson JM, DesRoches CM, Pollard WE, Parvanta C, Herrmann MJ. The Impact of Anthrax Attacks on the American Public. MedGenMed. 2002; 4:1. [PubMed: 12145561]
3. Okware SI, Omaswa FG, Zaramba S, Opio A, Lutwama JJ, Kamugisha J, Rwaguma EB, Kagwa P, Lamunu M. An Outbreak of Ebola in Uganda. Trop Med Int Health. 2002; 7:1068–75. [PubMed: 12460399]
4. Nkoghe D, Kone ML, Yada A, Leroy E. A Limited Outbreak of Ebola Haemorrhagic Fever in Etoumbi, Republic of Congo, 2005. Trans R Soc Trop Med Hyg. 2011; 105:466–72. [PubMed: 21605882]
5. Zhu H, Isikman SO, Mudanyali O, Greenbaum A, Ozcan A. Optical Imaging Techniques for Point-of-Care Diagnostics. Lab Chip. 2012; 13:51–67. [PubMed: 23044793]
6. Formenty P, Leroy EM, Epelboin A, Libama F, Lenzi M, Sudeck H, Yaba P, Allarangar Y, Boumandouki P, Nkounkou VB, et al. Detection of Ebola Virus in Oral Fluid Specimens During Outbreaks of Ebola Virus Hemorrhagic Fever in the Republic of Congo. Clin Infect Dis. 2006; 42:1521–6. [PubMed: 16652308]
7. Towner JS, Khristova ML, Sealy TK, Vincent MJ, Erickson BR, Bawiec DA, Hartman AL, Comer JA, Zaki SR, Stroher U, et al. Marburgvirus Genomics and Association with a Large Hemorrhagic Fever Outbreak in Angola. J Virol. 2006; 80:6497–516. [PubMed: 16775337]
8. Towner JS, Sealy TK, Khristova ML, Albarino CG, Conlan S, Reeder SA, Quan PL, Lipkin WI, Downing R, Tappero JW, et al. Newly Discovered Ebola Virus Associated with Hemorrhagic Fever Outbreak in Uganda. PLoS Pathog. 2008; 4:e1000212. [PubMed: 19023410]
9. Overend C, Yuan L, Peccoud J. The Synthetic Futures of Vesicular Stomatitis Virus. Trends Biotechnol. 2012; 30:497–8. [PubMed: 22789133]
10. Hastie E, Grdzelishvili VZ. Vesicular Stomatitis Virus as a Flexible Platform for Oncolytic Virotherapy Against Cancer. J Gen Virol. 2012; 93:2529–45. [PubMed: 23052398]
11. Lichty BD, Power AT, Stojdl DF, Bell JC. Vesicular Stomatitis Virus: Re-Inventing the Bullet. Trends Mol Med. 2004; 10:210–6. [PubMed: 15121047]
12. Meshii N, Takahashi G, Okunaga S, Hamada M, Iwai S, Takasu A, Ogawa Y, Yura Y. Enhancement of Systemic Tumor Immunity for Squamous Cell Carcinoma Cells by an Oncolytic Herpes Simplex Virus. Cancer Gene Ther. 2013
13. Angarita FA, Acuna SA, Ottolino-Perry K, Zerhouni S, McCart JA. Mounting a Strategic Offense: Fighting Tumor Vasculature with Oncolytic Viruses. Trends Mol Med. 2013; 19:378–92. [PubMed: 23540715]
14. Geisbert TW, Feldmann H. Recombinant Vesicular Stomatitis Virus-Based Vaccines Against Ebola and Marburg Virus Infections. J Infect Dis. 2011; 204(Suppl 3):S1075–81. [PubMed: 21987744]
15. Matsuura Y, Tani H, Komoda Y, Matsuo E, Suzuki K, Hamamoto I, Yamashita T, Moriishi K, Fujiyama K, Kanto T, et al. Replication-Competent Recombinant Vesicular Stomatitis Virus Encoding Hepatitis C Virus Envelope Proteins. Journal of Virology. 2007; 81:8601–8612. [PubMed: 17553880]
16. Geisbert TW, Daddario-DiCaprio KM, Lewis MG, Geisbert JB, Grolla A, Leung A, Paragas J, Matthias L, Smith MA, Jones SM, et al. Vesicular Stomatitis Virus-Based Ebola Vaccine is Well-Tolerated and Protects Immunocompromised Nonhuman Primates. Plos Pathogens. 2008; 4
17. Amann R, Rohde J, Wulle U, Conlee D, Raue R, Martinon O, Rziha HJ. A New Rabies Vaccine Based on a Recombinant ORF Virus (Parapoxvirus) Expressing the Rabies Virus Glycoprotein. J Virol. 2012; 87:1618–30. [PubMed: 23175365]
18. Shi J, Votruba AR, Farokhzad OC, Langer R. Nanotechnology in Drug Delivery and Tissue Engineering: From Discovery to Applications. Nano Lett. 2010; 10:3223–30. [PubMed: 20726522]
19. Jain RK, Stylianopoulos T. Delivering Nanomedicine to Solid Tumors. Nat Rev Clin Oncol. 2010; 7:653–64. [PubMed: 20838415]
20. Yurt A, Daaboul GG, Connor JH, Goldberg BB, Unlu MS. Single Nanoparticle Detectors for Biological Applications. Nanoscale. 2012; 4:715–726. [PubMed: 22214976]

21. Chantada L, Nikolaev NI, Ivanov AL, Borri P, Langbein W. Optical Resonances in Microcylinders: Response to Perturbations for Biosensing. Journal of the Optical Society of America B-Optical Physics. 2008; 25:1312–1321.
22. Lee J, Shen W, Payer K, Burg TP, Manalis SR. Toward Attogram Mass Measurements in Solution with Suspended Nanochannel Resonators. Nano Lett. 2010; 10:2537–42. [PubMed: 20527897]
23. Burg TP, Godin M, Knudsen SM, Shen W, Carlson G, Foster JS, Babcock K, Manalis SR. Weighing of Biomolecules, Single Cells and Single Nanoparticles in Fluid. Nature. 2007; 446:1066–9. [PubMed: 17460669]
24. Fraikin JL, Teesalu T, McKenney CM, Ruoslahti E, Cleland AN. A High-Throughput Label-Free Nanoparticle Analyser. Nature Nanotechnology. 2011; 6:308–313.
25. Mudanyali O, McLeod E, Luo W, Greenbaum A, Coskun AF, Hennequin Y, Allier CP, Ozcan A. Wide-Field Optical Detection of Nanoparticles Using On-Chip Microscopy and Self-Assembled Nanolenses. Nat Photonics. :7.
26. Wei Q, Qi H, Luo W, Tseng D, Ki SJ, Wan Z, Gorocs Z, Bentolila LA, Wu TT, Sun R, et al. Fluorescent Imaging of Single Nanoparticles and Viruses on a Smart Phone. Acs Nano. 7:9147–55. [PubMed: 24016065]
27. Daaboul GG, Lopez CA, Yurt A, Goldberg B, Connor JH, Unlu MS. Label-Free Optical Biosensors for Virus Detection and Characterization. Selected Topics in Quantum Electronics, IEEE. 2012; 18:1422–33.
28. Daaboul GG, Yurt A, Zhang X, Hwang GM, Goldberg BB, Unlu MS. High-Throughput Detection and Sizing of Individual Low-Index Nanoparticles and Viruses for Pathogen Identification. Nano Letters. 2010; 10:4727–4731. [PubMed: 20964282]
29. Cretich M, Pirri G, Damin F, Solinas I, Chiari M. A New Polymeric Coating for Protein Microarrays. Analytical Biochemistry. 2004; 332:67–74. [PubMed: 15301950]
30. Murphy, FA.; Harrison, AK. Electron Microscopy of the Rhabdoviruses of Animals. Vol. 1. CRC Press; Boca Raton: 1980. p. 65-106.
31. Ge P, Tsao J, Schein S, Green TJ, Luo M, Zhou ZH. Cryo-EM Model of the Bullet-Shaped Vesicular Stomatitis Virus. Science. 327:689–93. [PubMed: 20133572]
32. Brown JC, Newcomb WW, Wertz GW. Helical Virus Structure: The Case of the Rhabdovirus Bullet. Viruses. 2:995–1001. [PubMed: 21994666]
33. Cave DR, Hendrickson FM, Huang AS. Defective Interfering Virus Particles Modulate Virulence. J Virol. 1985; 55:366–73. [PubMed: 2991562]
34. Thompson KA, Yin J. Population Dynamics of an RNA Virus and its Defective Interfering Particles in Passage Cultures. Virol J. 2010; 7:257. [PubMed: 20920247]
35. Li D, Lott WB, Lowry K, Jones A, Thu HM, Aaskov J. Defective Interfering Viral Particles in Acute Dengue Infections. PLoS One. 2011; 6:e19447. [PubMed: 21559384]
36. Falzarano D, Feldmann F, Grolla A, Leung A, Ebihara H, Strong JE, Marzi A, Takada A, Jones S, Gren J, et al. Single Immunization with a Monovalent Vesicular Stomatitis Virus-Based Vaccine Protects Nonhuman Primates Against Heterologous Challenge with Bundibugyo Ebolavirus. J Infect Dis. 2011; 204(Suppl 3):S1082–9. [PubMed: 21987745]
37. Geisbert TW, Daddario-Dicaprio KM, Geisbert JB, Reed DS, Feldmann F, Grolla A, Stroher U, Fritz EA, Hensley LE, Jones SM, et al. Vesicular Stomatitis Virus-Based Vaccines Protect Nonhuman Primates Against Aerosol Challenge with Ebola and Marburg Viruses. Vaccine. 2008; 26:6894–900. [PubMed: 18930776]
38. Geisbert TW, Daddario-Dicaprio KM, Lewis MG, Geisbert JB, Grolla A, Leung A, Paragas J, Matthias L, Smith MA, Jones SM, et al. Vesicular Stomatitis Virus-Based Ebola Vaccine is Well-Tolerated and Protects Immunocompromised Nonhuman Primates. PLoS Pathog. 2008; 4:e1000225. [PubMed: 19043556]
39. Geisbert TW, Daddario-DiCaprio KM, Williams KJN, Geisbert JB, Leung A, Feldmann F, Hensley LE, Feldmann H, Jones SM. Recombinant Vesicular Stomatitis Virus Vector Mediates Postexposure Protection Against Sudan Ebola Hemorrhagic Fever in Nonhuman Primates. Journal of Virology. 2008; 82:5664–5668. [PubMed: 18385248]

40. Marzi A, Ebihara H, Callison J, Groseth A, Williams KJ, Geisbert TW, Feldmann H. Vesicular Stomatitis Virus-Based Ebola Vaccines with Improved Cross-Protective Efficacy. J Infect Dis. 2011; 204(Suppl 3):S1066–74. [PubMed: 21987743]

41. Marzi A, Feldmann H, Geisbert TW, Falzarano D. Vesicular Stomatitis Virus-Based Vaccines for Prophylaxis and Treatment of Filovirus Infections. J Bioterror Biodef. 2012:S1.

42. Mire CE, Miller AD, Carville A, Westmoreland SV, Geisbert JB, Mansfield KG, Feldmann H, Hensley LE, Geisbert TW. Recombinant Vesicular Stomatitis Virus Vaccine Vectors Expressing Filovirus Glycoproteins Lack Neurovirulence in Nonhuman Primates. PLoS Negl Trop Dis. 2012; 6:e1567. [PubMed: 22448291]

43. Ksiazek TG, Rollin PE, Jahrling PB, Johnson E, Dalgard DW, Peters CJ. Enzyme Immunosorbent Assay for Ebola Virus Antigens in Tissues of Infected Primates. J Clin Microbiol. 1992; 30:947–50. [PubMed: 1572982]

44. Towner JS, Rollin PE, Bausch DG, Sanchez A, Crary SM, Vincent M, Lee WF, Spiropoulou CF, Ksiazek TG, Lukwiya M, et al. Rapid Diagnosis of Ebola Hemorrhagic Fever by Reverse Transcription-PCR in an Outbreak Setting and Assessment of Patient Viral Load as a Predictor of Outcome. J Virol. 2004; 78:4330–41. [PubMed: 15047846]

45. Wolf P. The Nature and Significance of Platelet Products in Human Plasma. Br J Haematol. 1967; 13:269–88. [PubMed: 6025241]

46. Sustar V, Bedina-Zavec A, Stukelj R, Frank M, Bobojevic G, Jansa R, Ogorevc E, Kruljc P, Mam K, Simunic B, et al. Nanoparticles Isolated from Blood: A Reflection of Vesiculability of Blood Cells During the Isolation Process. Int J Nanomedicine. 2011; 6:2737–48. [PubMed: 22128248]

47. Simak J, Gelderman MP. Cell Membrane Microparticles in Blood and Blood Products: Potentially Pathogenic Agents and Diagnostic Markers. Transfus Med Rev. 2006; 20:1–26. [PubMed: 16373184]

48. Lundqvist M, Stigler J, Elia G, Lynch I, Cedervall T, Dawson KA. Nanoparticle Size and Surface Properties Determine the Protein Corona with Possible Implications for Biological Impacts. Proc Natl Acad Sci U S A. 2008; 105:14265–70. [PubMed: 18809927]

49. Anabousi S, Bakowsky U, Schneider M, Huwer H, Lehr CM, Ehrhardt C. *In Vitro* Assessment of Transferrin-Conjugated Liposomes as Drug Delivery Systems for Inhalation Therapy of Lung Cancer. Eur J Pharm Sci. 2006; 29:367–74. [PubMed: 16952451]

50. Reddington AP, Trueb JT, Freedman DS, Tuysuzoglu A, Daaboul GG, Lopez CA, Karl WC, Connor JH, Fawcett H, Unlu MS. An Interferometric Reflectance Imaging Sensor for Point of Care Viral Diagnostics. IEEE Transactions on Biomedical Engineering. 2013; 60:3276–3283. [PubMed: 24271115]

51. Whitt MA. Generation of VSV Pseudotypes Using Recombinant DeltaG-VSV for Studies on Virus Entry, Identification of Entry Inhibitors, and Immune Responses to Vaccines. J Virol Methods. 2010; 169:365–74. [PubMed: 20709108]

52. Garbutt M, Liebscher R, Wahl-Jensen V, Jones S, Moller P, Wagner R, Volchkov V, Klenk HD, Feldmann H, Stroher U. Properties of Replication-Competent Vesicular Stomatitis Virus Vectors Expressing Glycoproteins of Filoviruses and Arenaviruses. J Virol. 2004; 78:5458–65. [PubMed: 15113924]

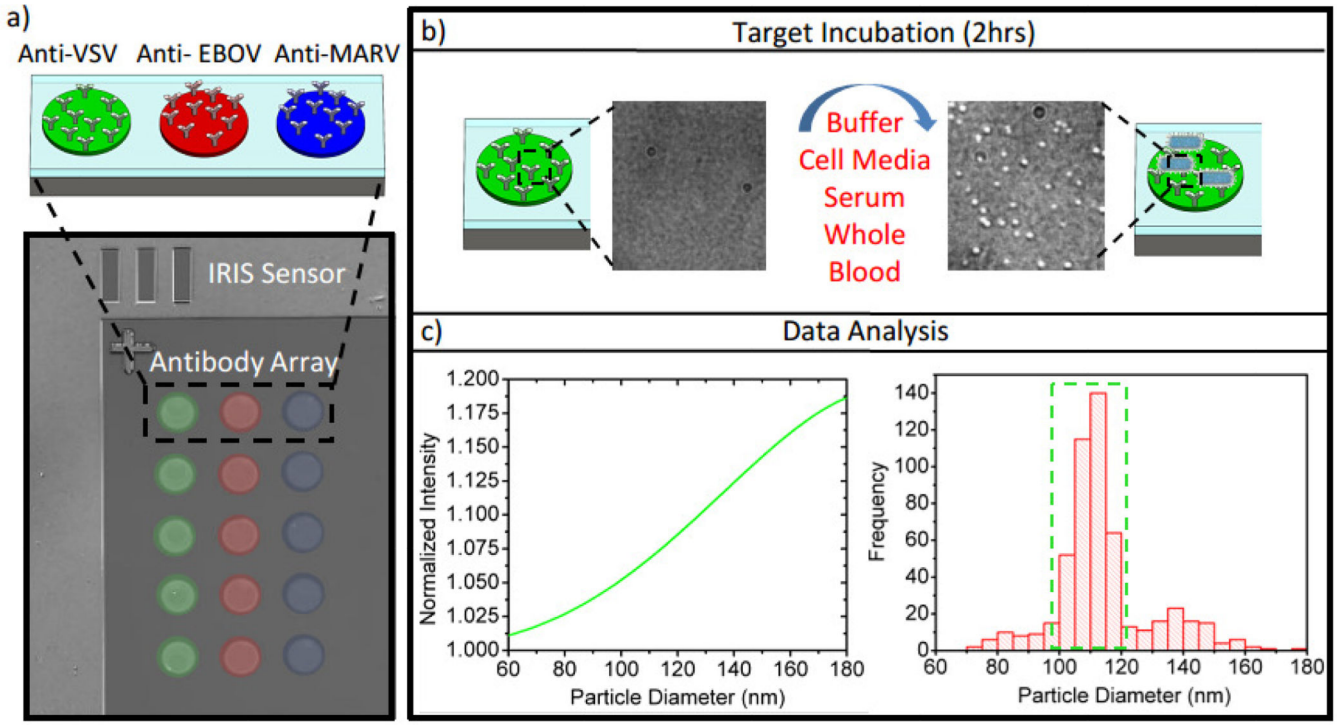

Figure 1.

Depiction of the microarray configuration and data acquisition and analysis processes for virus identification using SP-IRIS. (a) Representative microarray of immobilized antibody spots prior to incubation. Green, red, and blue spots represent anti-VSV, anti-EBOV, and anti-MARV probes, respectively. (b) Post-incubation images for anti-VSV spots show increased particle counts (right) as compared to pre-incubation images (left). (c) A previously validated sizing model (left) is used to determine the size of each particle within the spot. A distribution of sizes (right) can then be produced from particles identified in each image. The region within the dashed rectangle represents the expected size window of VSV and the filter chosen to remove background particles. By comparing particles found within the expected virus size range for pre- and post-incubation images, individual virions can be identified and counted.

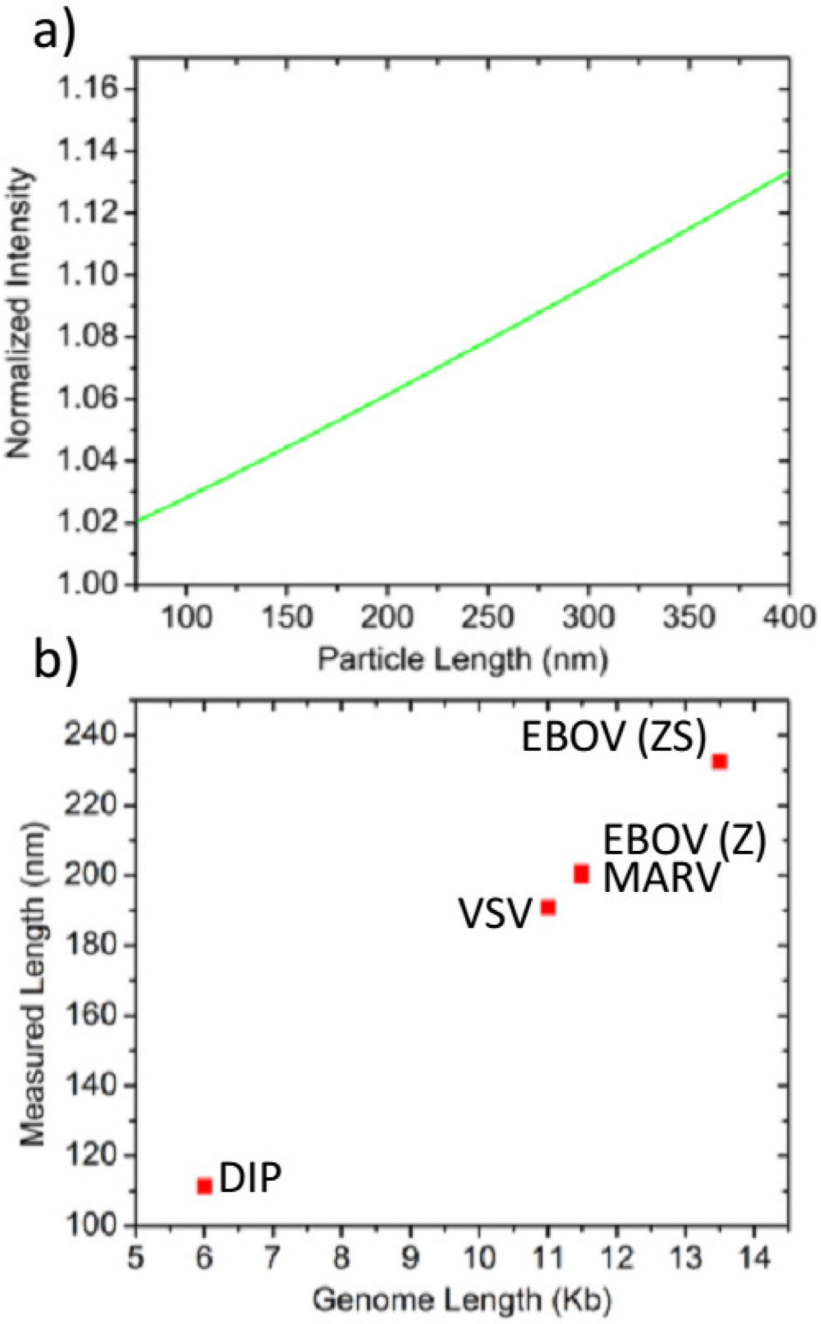

Figure 2.

Virus characterization based on genome length and glycoprotein expression. (a) SP-IRIS calculated response curve for a cylindrical particle with a fixed width of 75 nm and varying length. The sizing curve is used to calculate the dimension of VSV-based virus particles bound to the sensor surface. (b) SP-IRIS measured virus length for DIP, VSV, MARV, EBOV-Zaire (Z), and EBOV-Zaire/Sudan (ZS) variants.

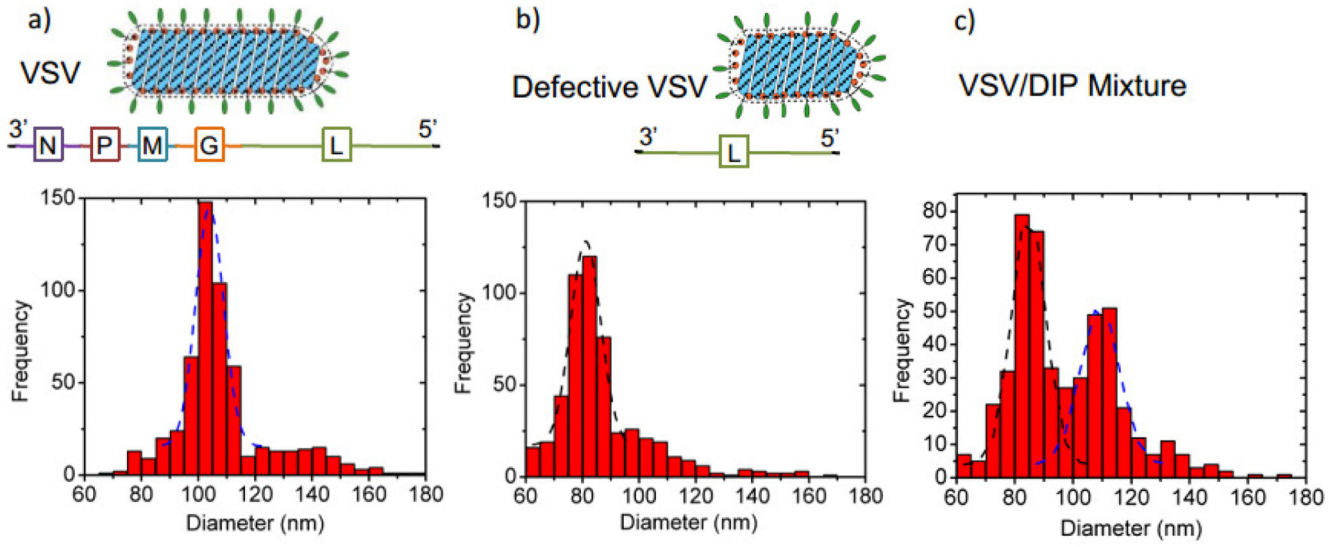

Figure 3.

Differentiation of VSV and DIP through particle size analysis. The size difference between VSV and DIP is caused by shortening of the genome. As shown in the figure, the DIP genome only codes for the L protein and is reduced by approximately 5 kb as compared to the wild type virus. (a) Sizing of wild type VSV bound to the SP-IRIS sensor. (b) Sizing of DIP bound to the SP-IRIS sensor. (c) Sizing of a mixture of wild type VSV and DIP captured on the sensor surface. Dashed lines represent a fitted Gaussian distribution to help guide the reader.

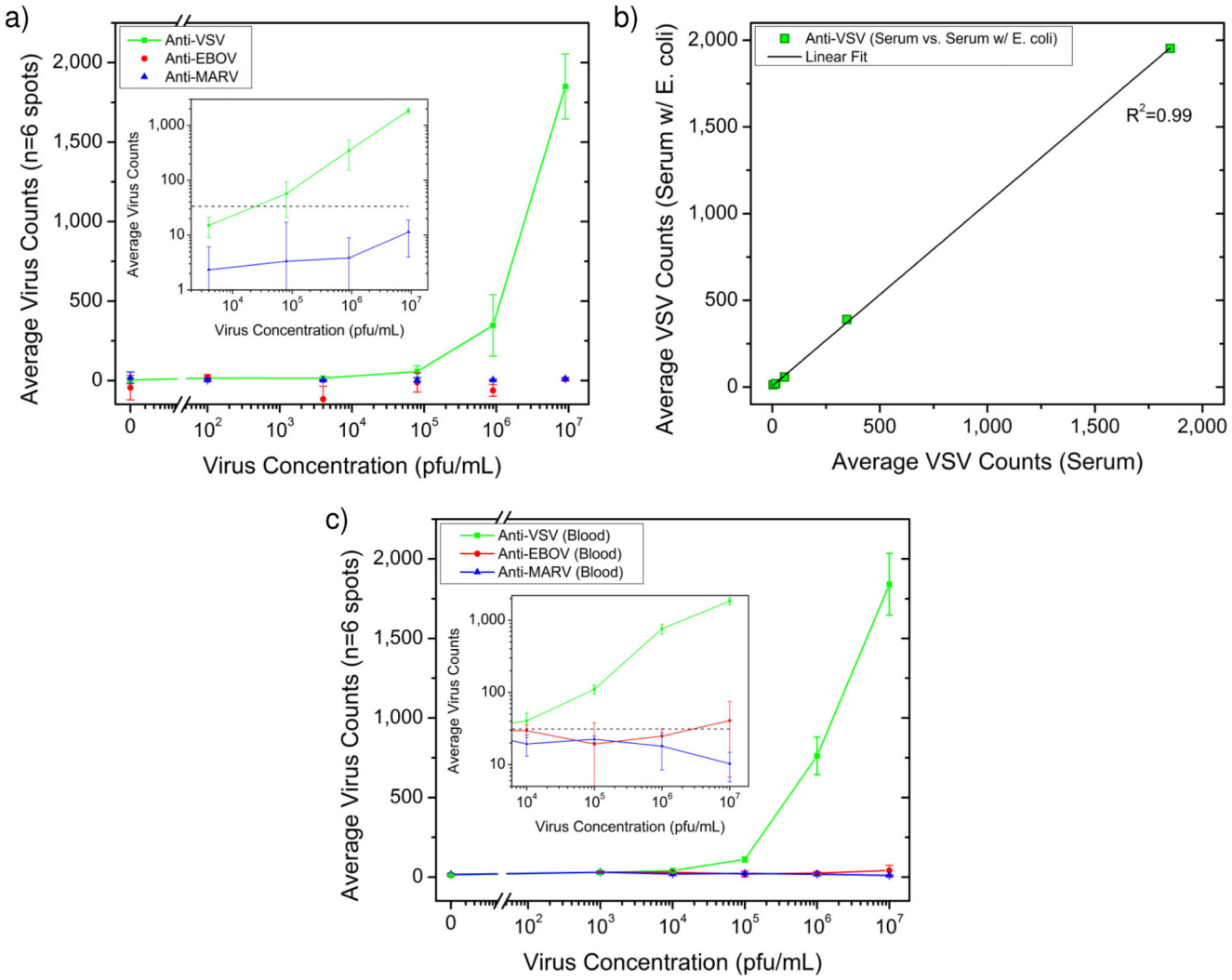

Figure 4.

Sensitivity analysis for wild type VSV diluted in 100% FBS. (a) The average virus counts (for n=6 replicate spots) were plotted against the plaque assay measured virus concentration for each condition. The inset shows a logarithmic plot for counts determined on anti-VSV and anti-MARV (control) spots for the same data. A limit-of-detection threshold (dashed line) was set based on the mean plus three standard deviations for the anti-VSV spots for the blank sample. (b) Nearly identical responses are observed for FBS samples that were deliberately contaminated with E. coli at high concentrations. (c) The response for VSV is unaffected for detection in whole blood-diluted samples. Similar virus counts were detected for the anti-VSV and control spots in blood as observed for serum dilutions. For (a) and (c), the lines connecting the data points are present only to guide the reader's eye, however in (b), the line represents a regression fit to the data.

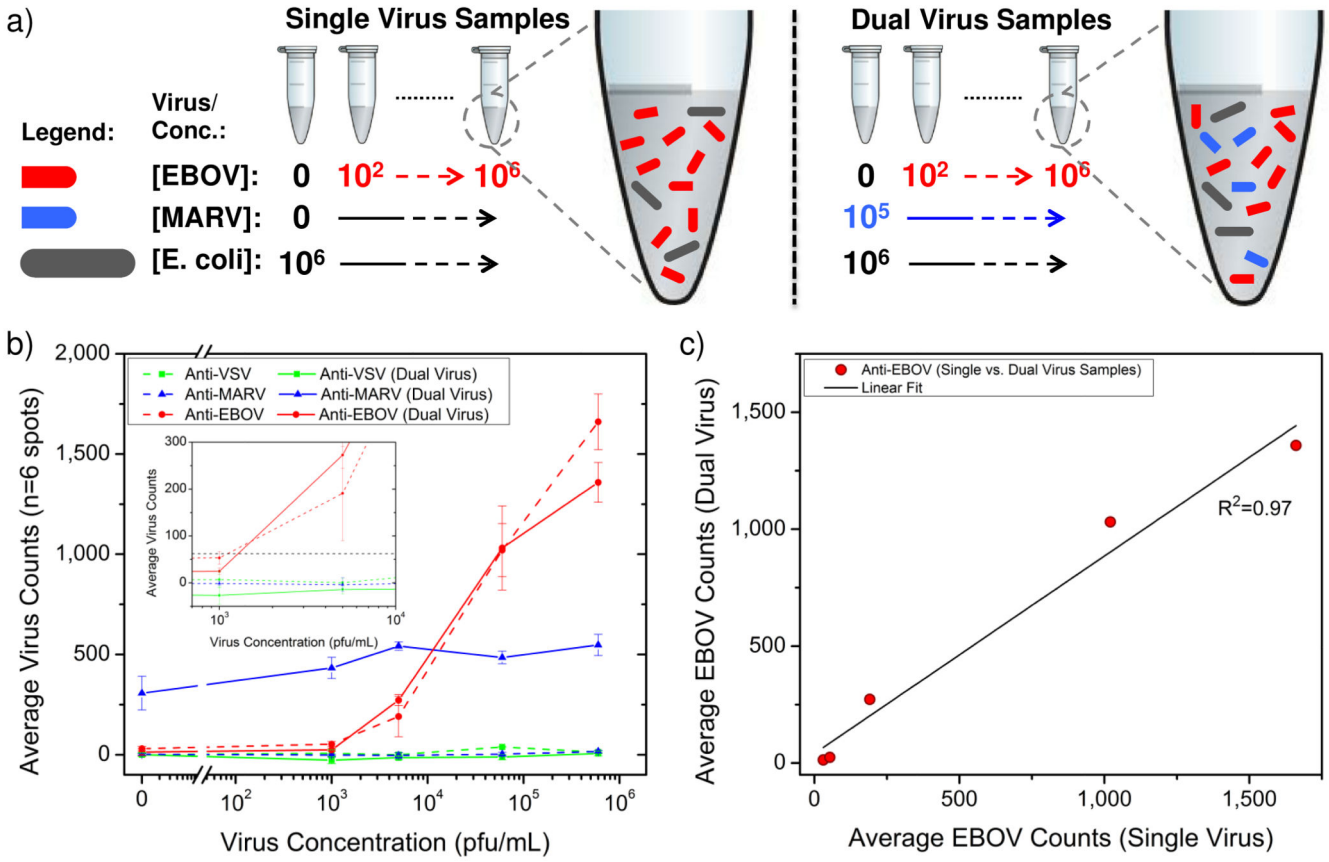

Figure 5.

Duplexed detection of Ebola and Marburg-pseudotyped viruses in regular serum and bacteria-laden samples. a) Schematic of sample preparation and contents. Both single and dual virus samples were made in serum containing 10^6 cfu/mL E. coli K12. b) In normal serum samples the exponential response observed for anti-Ebola spots was similar to detection for VSV. Sensor substrates that were incubated in the bacteria-laden samples showed nearly identical responses for the titrated Ebola pseudotype concentration, however the presence of the Marburg pseudotype at constant concentration produced an additional signal for the anti-Marburg spots for all samples. The inset shows an expanded view of concentrations around 10^3 pfu/mL; the dashed line represents the detection threshold estimated from the mean plus three standard deviations for the ant-Ebola spots incubated in the FBS blank sample. Again, for b) the lines connecting the data points are present only to guide the reader's eye between single and dual virus sample responses. c) The response observed between the anti-Ebola spots in normal FBS and bacteria-containing samples was similar as shown by the linear regression fit to a scatter plot of one sample type against the other.